Li and Jiao, https://doi.org/10.1083/jcb.201610014

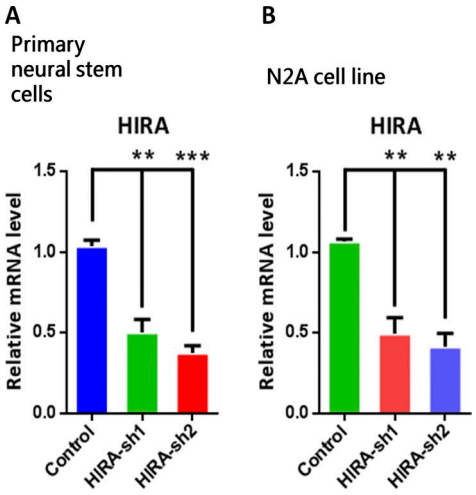

Figure S1. **Real-time PCR detection of HIRA knockdown efficiency.** (A) NPCs isolated from E12.5 cortex were cultured for 24 h and infected with control or HIRA shRNA lentiviruses. RNA was extracted 3 d later and used for reverse transcription into cDNA. Finally, the cDNA was used for real-time PCR analysis (n = 3; mean ± SEM; **, P < 0.01; ***, P < 0.001; t test, two sided). (B) N2A cells were transfected with control or HIRA shRNA plasmids. RNA was extracted 3 d later and used for reverse transcription into cDNA. Finally, the cDNA was used for real-time PCR analysis (n = 4; mean ± SEM; **, P < 0.01; t test, two sided).

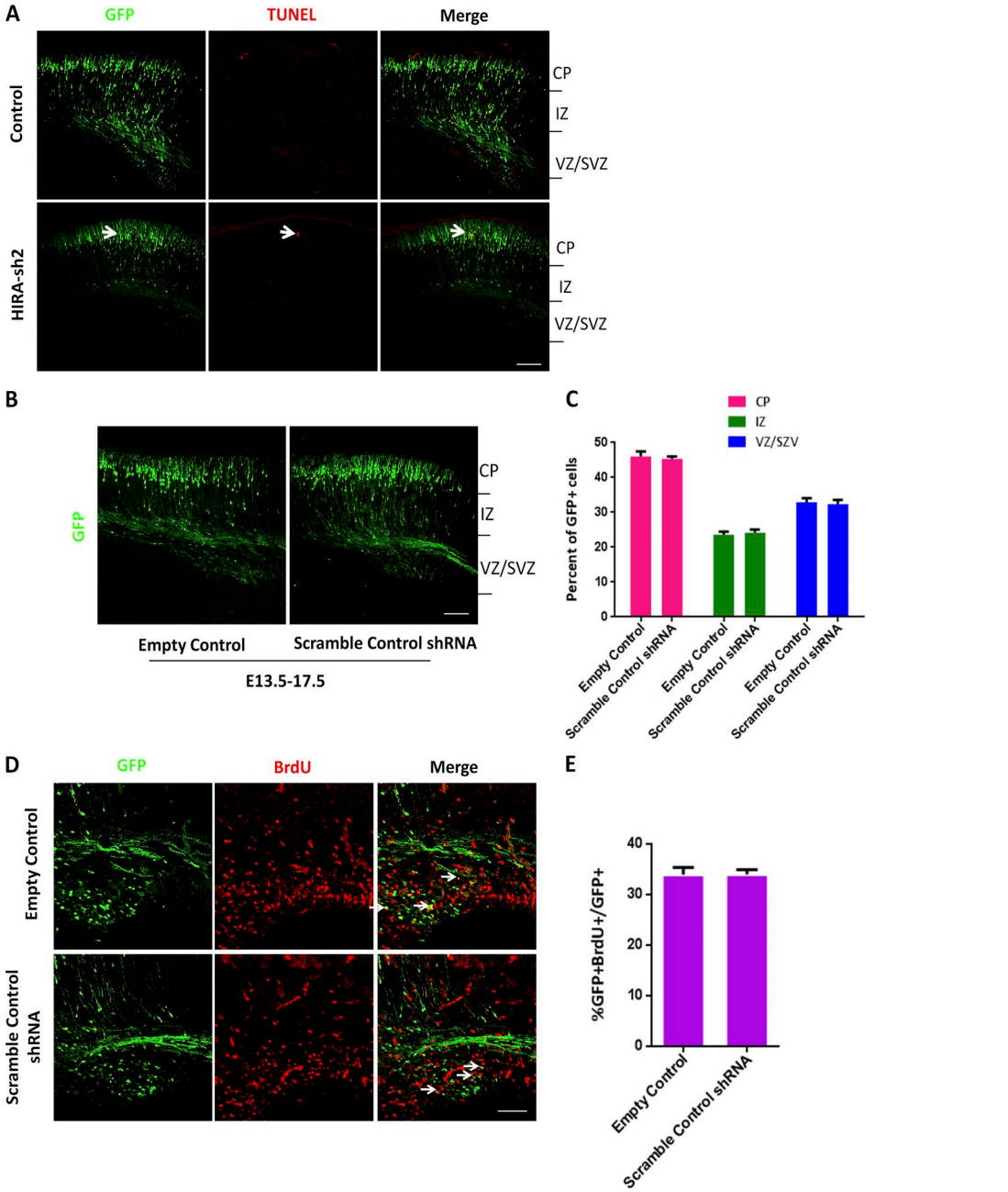

Figure S2. **HIRA knockdown has no effect on NPC apoptosis, and there is little difference in the positioning of GFP-positive cells between the scrambled control shRNA and empty control shRNA groups.** (A) The ratio of GFP and TUNEL double-positive cells does not change in HIRA-silenced brains compared with controls. Control or HIRA-sh2 plasmids were electroporated into E13.5 embryonic mouse brains, and mice were sacrificed at E17.5. Bar, 50 µm. (B and C) The positioning of GFP-positive cells in the scrambled control shRNA group is similar with that in the empty control shRNA group. Empty control or the scrambled control shRNA plasmids were electroporated into E13.5 embryonic mouse brains, and mice were sacrificed at E17.5. The percentage of GFP-positive cells in each region was quantified (n = 3; mean ± SEM ; t test, two sided). Bar, 50 µm. (D and E) The ratio of BrdU and GFP double-positive cells are similar in the empty control shRNA and the scrambled control shRNA groups. The brains were electroporated at E13.5, and 100 mg/kg BrdU was injected i.p. into pregnant mice 2 h before the collection of embryos at E17.5. The arrows indicate GFP/BrdU double-positive cells. The bar graph displays the percentage of GFP/BrdU double-positive cells relative to the total number of GFP-positive cells in the VZ/SVZ (n = 3; mean ± SEM ; t test, two sided). Bar, 20 µm. IZ, intermediate zone.

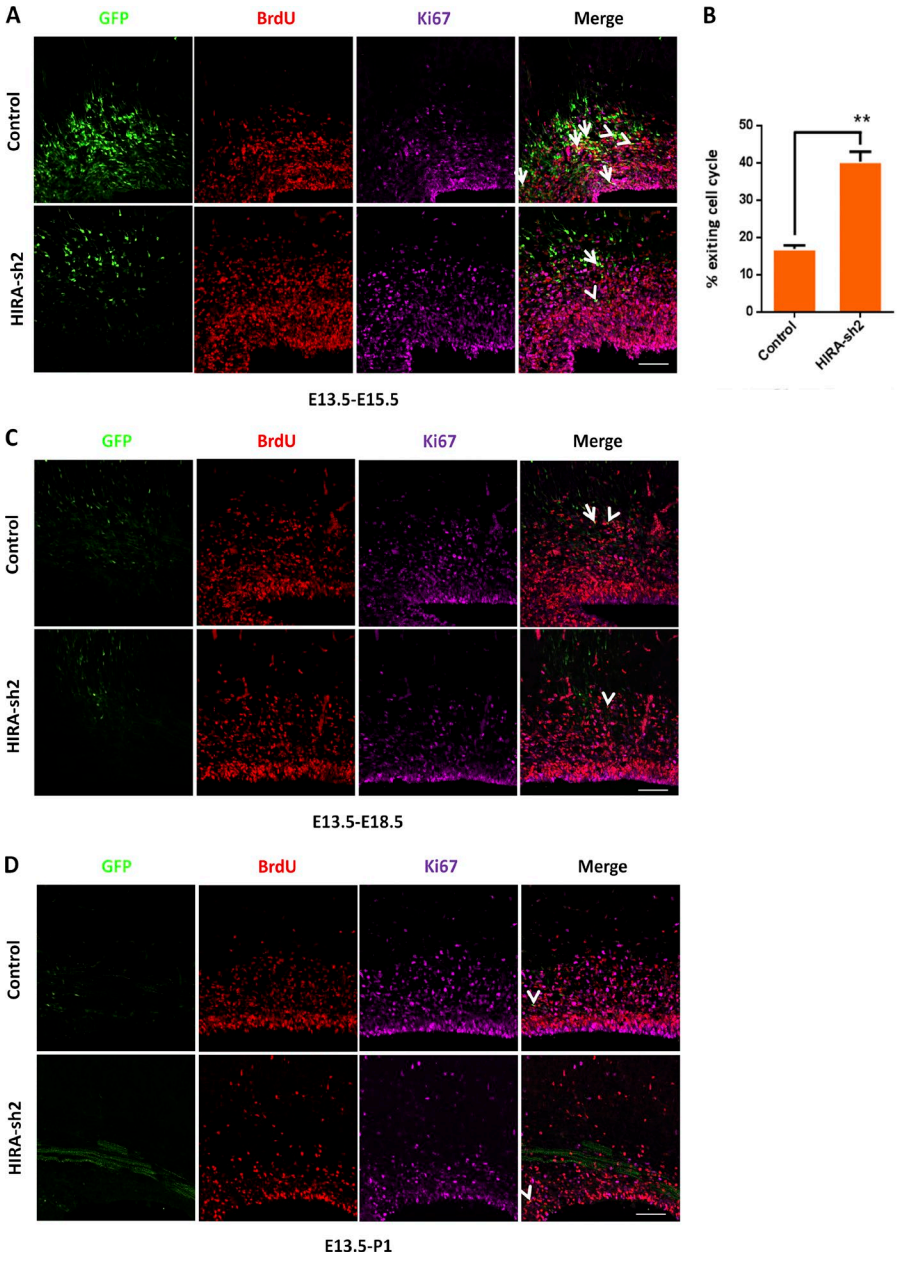

Figure S3. **Down-regulation of HIRA promotes cell cycle exit.** (A and B) Control or HIRA shRNA plasmids were electroporated into E13.5 mouse brains, and BrdU was injected at E14.5. At E15.5, embryonic brains were collected for analysis of immunohistochemistry using anti–BrdU and anti–Ki67 antibodies. The cell cycle exit index is calculated by the percentage of GFP-positive cells that exited the cell cycle ($GFP^+BrdU^+Ki67^-$) divided by the total GFP and BrdU double-positive (GFP^+BrdU^+) cells. Arrows represent $GFP^+BrdU^+Ki67^+$ cells, and arrowheads represent $GFP^+BrdU^+Ki67^-$ cells. The bar graph shows the percentage of $GFP^+BrdU^+Ki67^-$ cells relative to the total BrdU and GFP double-positive cells in the VZ/SVZ ($n = 3$; mean ± SEM; **, $P < 0.01$; *t* test, two sided). Bar, 20 µm. (C) Control or HIRA shRNA plasmids were electroporated into E13.5 mouse brains, and BrdU was injected at E17.5. At E18.5, the embryonic brains were collected for analysis of immunohistochemistry using anti–BrdU and anti–Ki67 antibodies. Arrowheads represent $GFP^+BrdU^+Ki67^-$ cells. Bar, 20 µm. (D) Control or HIRA shRNA plasmids were electroporated into E13.5 mouse brains, and BrdU was injected at P0. At P1, embryonic brains were collected for analysis of immunohistochemistry using anti-BrdU and -Ki67 antibodies. Arrowheads represent $GFP^+BrdU^+Ki67^-$ cells. Bar, 20 µm.

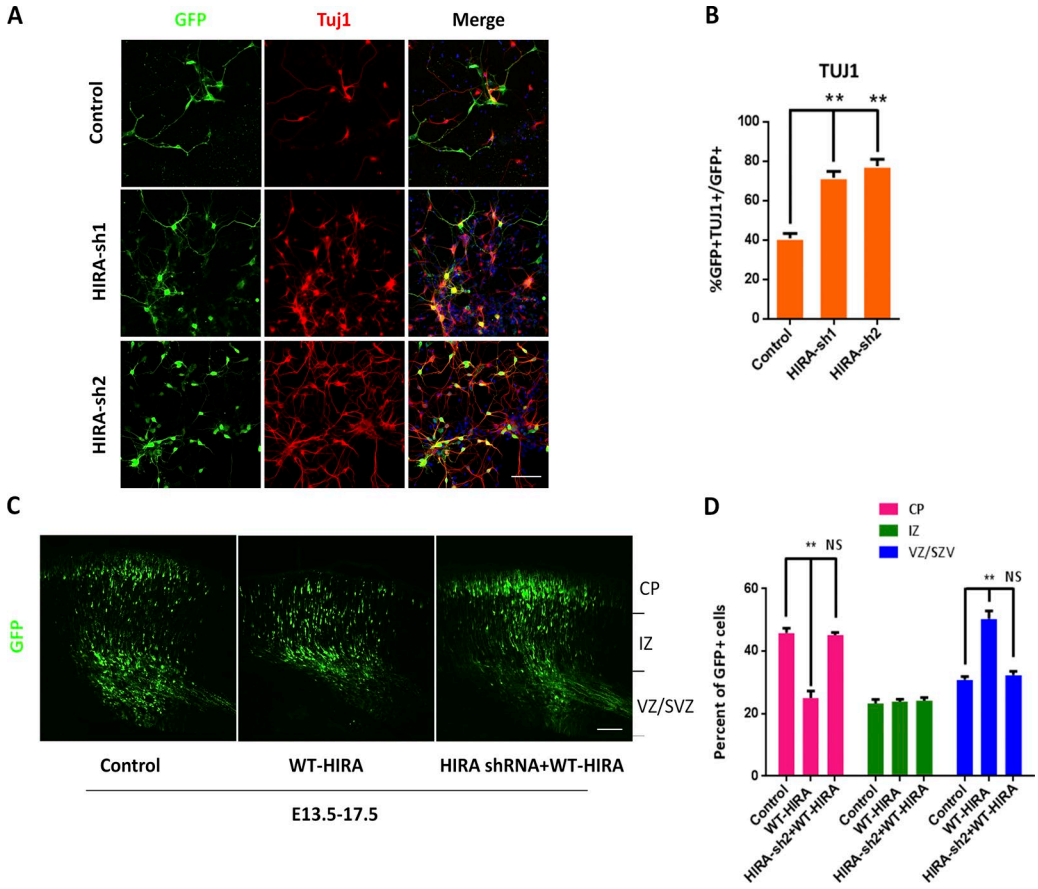

Figure S4. **HIRA knockdown increases differentiation in vitro.** (A and B) HIRA knockdown increases the ratio of GFP and TUJ1 double-positive cells in vitro. The isolated NPCs were infected with control, HIRA-sh1, or HIRA-sh2 lentiviruses and stained for TUJ1 3 d later. The bar graph exhibits the percentage of GFP and TUJ1 double-positive cells relative to total GFP-positive cells (n = 3; mean ± SEM; **, P < 0.01; t test, two sided). Bar, 25 µm. (C and D) Overexpression of HIRA rescues the positioning defects caused by HIRA knockdown in vivo. Control, WT-HIRA, and HIRA-sh2 together with WT-HIRA plasmids were electroporated into E13.5 embryonic mouse brains, and embryos were sacrificed at E17.5 for phenotypic analysis. The percentage of GFP-positive cells in each region is exhibited (n = 3; mean ± SEM; **, P < 0.01; NS, not significant; t test, two sided). Bar, 50 µm. IZ, intermediate zone.

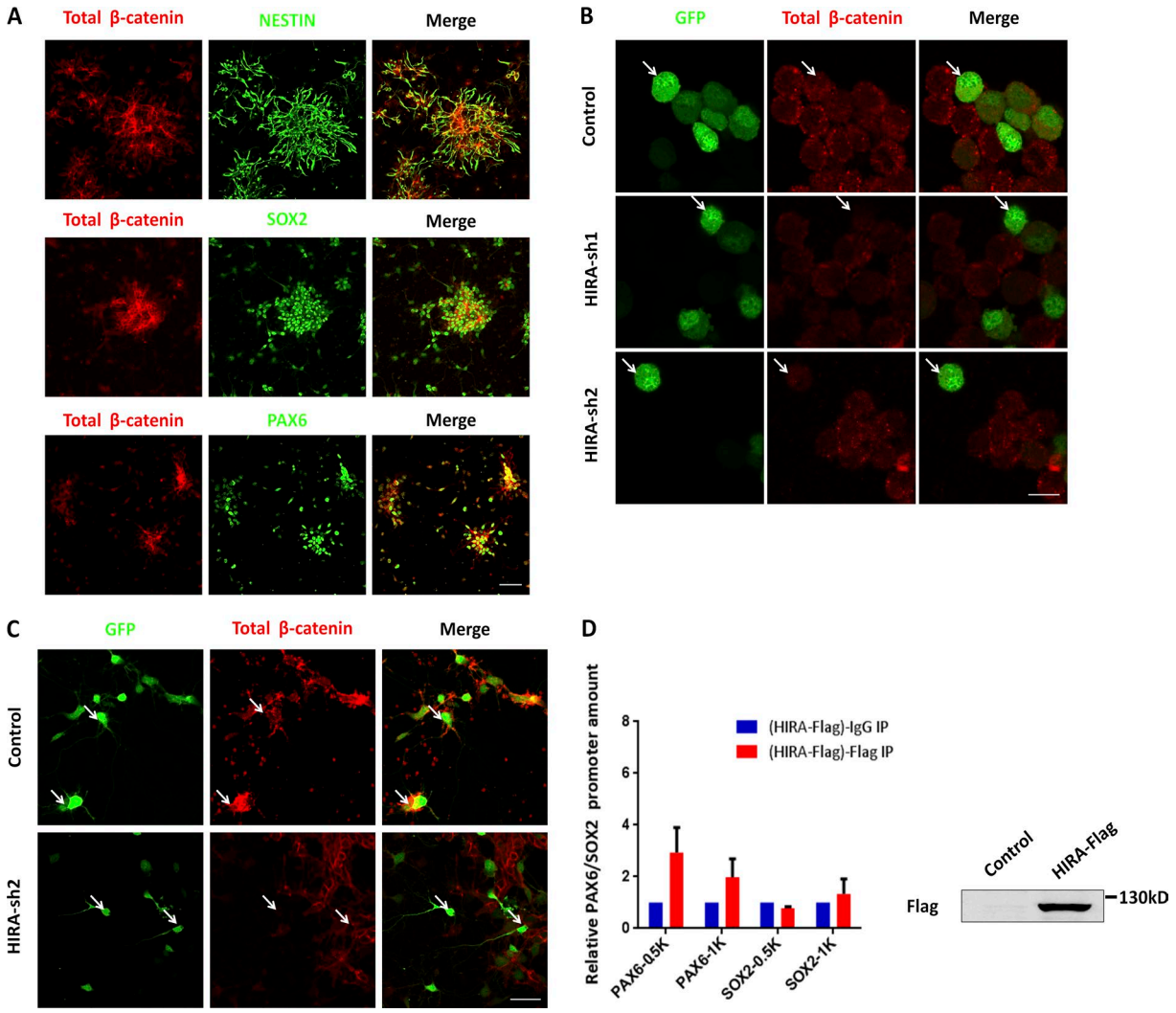

Figure S5. **β-Catenin is enriched in isolated NPCs, and HIRA knockdown reduces β-catenin in vitro.** (A) NPCs were isolated from the E12.5 mice brains and cultured in the proliferative medium for 1 d. Subsequently, the cells were costained for total β-catenin and NESTIN, total β-catenin and SOX2, and total β-catenin and PAX6, respectively. Bar, 25 μm. (B) HIRA knockdown decreases β-catenin-GFP double-positive cells in N2A cells. N2A cells were transfected with control or HIRA shRNAs plasmids. Cells were stained for total β-catenin. The arrows show some GFP-positive cells. Bar, 15 μm. (C) HIRA knockdown reduces β-catenin-GFP double-positive cells in NPCs. NPCs isolated from E12.5 cortex were cultured for 24 h and infected with control or HIRA-sh2 lentiviruses. Cells were stained for total β-catenin 3 d later. The arrows show some GFP-positive cells. Bar, 25 μm. (D) The effect of HIRA to PAX6/SOX2 promoter. The binding of HIRA to PAX6 or SOX2 promoter was determined through ChIP and real-time PCR (n = 3; mean ± SEM).

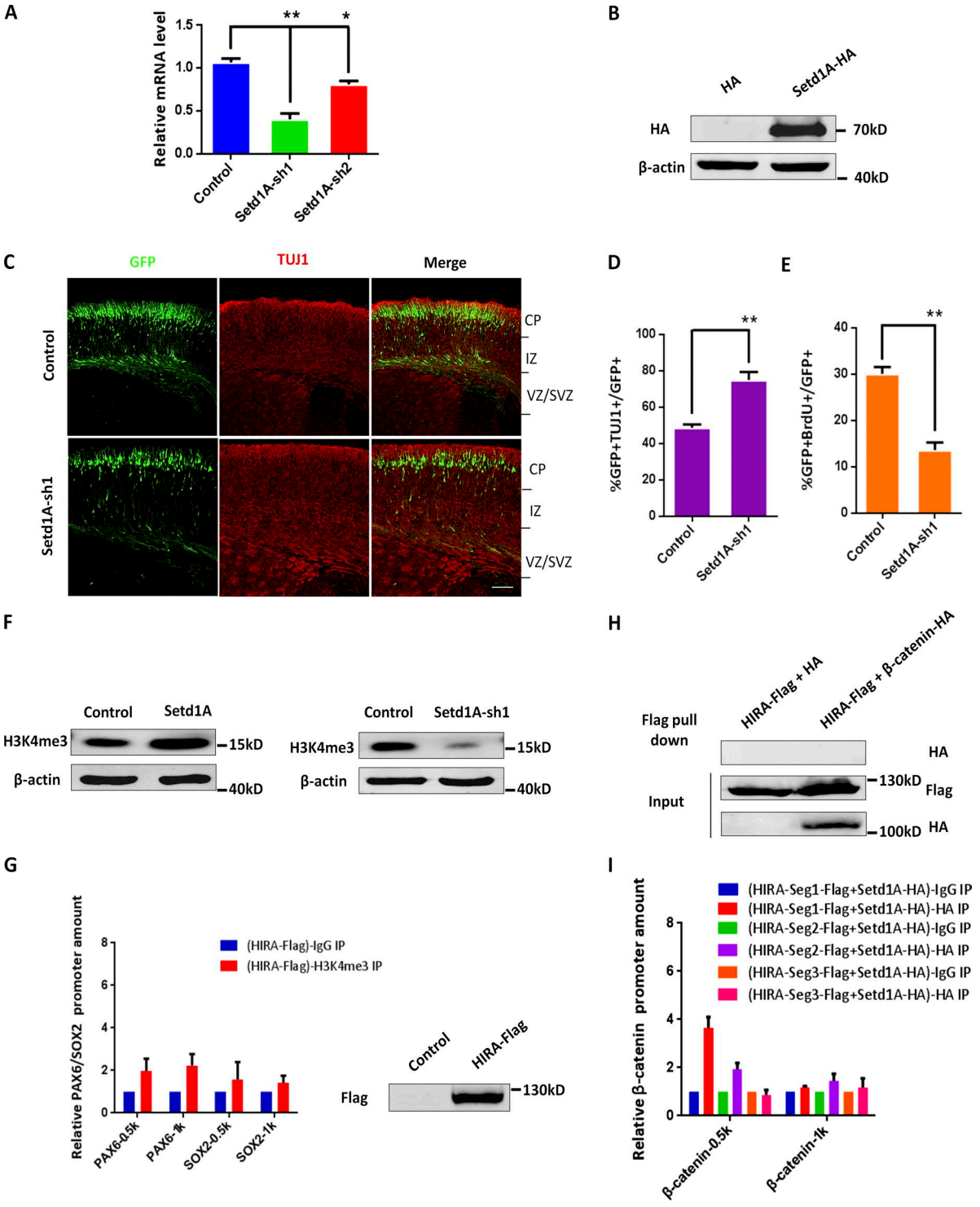

Figure S6. **Setd1A knockdown reduces proliferation and promotes differentiation of NPCs in utero.** (A) RT-PCR analysis shows the knockdown of Setd1A in NPCs (n = 3; mean ± SEM; *, P < 0.05; **, P < 0.01; t test, two sided). (B) Western blot analysis shows the overexpression of Setd1A in NPCs. β-actin was used as a loading control. (C and D) HIRA knockdown increases the ratio of GFP and TUJ1 double-positive cells in utero. E17.5 brain sections were stained for TUJ1 after the electroporation of control or Setd1A-sh1 plasmids into the brain at E13.5. The percentage of GFP and TUJ1 double-positive cells relative to the total GFP-positive cells is displayed as a bar graph (n = 3; mean ± SEM; **, P < 0.01; t test, two sided). Bar, 50 µm. IZ, intermediate zone. (E) The bar graph displays the percentage of GFP/BrdU double-positive cells relative to the total GFP-positive cells in the VZ/SVZ (n = 3; mean ± SEM; **, P < 0.01; t test, two sided). (F) Western blot analysis of the protein level of H3K4me3 when NPCs cultured in vitro were infected with control, Setd1A, or Setd1A-sh1 lentiviruses. β-Actin was used as a loading control (n = 3). (G) H3K4me3 deposition at the PAX6 or SOX2 locus upon HIRA overexpression. The binding of H3K4me3 to the PAX6 or SOX2 promoter was determined through ChIP and real-time PCR (n = 3; mean ± SEM). The anti–H3K4me3 antibody was used for immunoprecipitation (IP). (H) HIRA and β-catenin have no interaction between each other in the protein level. The immunoprecipitated proteins were probed with anti–Flag antibodies to detect Flag-HIRA. N2A cells were used in this experiment (n = 3). (I) Primary NPCs were infected with Setd1A-HA together with HIRA-Seg1-Flag, Setd1A-HA together with HIRA-Seg2-Flag, or Setd1A-HA together with HIRA-Seg3-Flag co-overexpression lentiviruses, and the anti–HA antibody was used for IP. Protein binding to the β-catenin promoter was determined through ChIP and real-time PCR (n = 3; mean ± SEM).

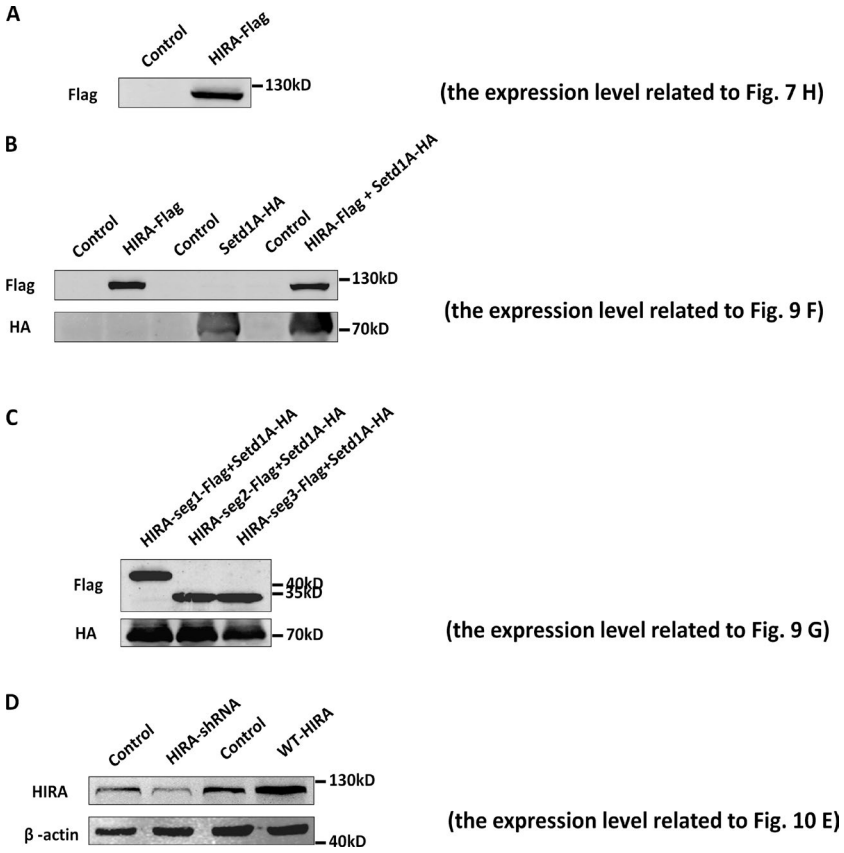

Figure S7. **Protein expression levels for ChIP assays.** (A) The Western blot result shows the expression level of HIRA in Fig. 7 H. (B) The Western blot result shows the expression level of HIRA and Setd1A in Fig. 9 F. (C) The Western blot result shows the expression level of HIRA and Setd1A in Fig. 9 G. (D) The Western blot result shows the expression level of HIRA in Fig.10 E.